

Strong saturation absorption imaging of dense clouds of ultracold atoms

G. Reinaudi,¹ T. Lahaye,^{1,2} Z. Wang,^{1,3} and D. Guéry-Odelin^{1,*}

¹Laboratoire Kastler Brossel, Ecole Normale Supérieure, 24 rue Lhomond, F-75231 Paris Cedex 05, France

²Physikalisches Institut, Universität Stuttgart, Pfaffenwaldring 57, D-70550 Stuttgart, Germany

³Institute of Optics, Department of Physics, Zhejiang University, Hangzhou 310027, China

*Corresponding author: dgo@lkb.ens.fr

Compiled October 23, 2018

We report on a far above saturation absorption imaging technique to investigate the characteristics of dense packets of ultracold atoms. The transparency of the cloud is controlled by the incident light intensity as a result of the non-linear response of the atoms to the probe beam. We detail our experimental procedure to calibrate the imaging system for reliable quantitative measurements, and demonstrate the use of this technique to extract the profile and its spatial extent of an optically thick atomic cloud. © 2018 Optical Society of America

OCIS codes: 110.0110, 020.7010

Recently there has been a resurgent interest in the production of dense samples [1,2] containing a large number of cold neutral atoms with highly compressed magneto-optical traps (MOT) [3,4]. These studies, combined with optical trapping, opened the way to a simplified and very rapid production of Bose-Einstein condensates [5], and may also play a key role in the production of a cw atom laser based on the periodical coupling of atomic packets into a magnetic guide, yielding a promising starting point for evaporative cooling [6].

For dense clouds, an important issue is the reliability of the method used to extract the atomic densities. The predominant imaging techniques for dilute samples, low-intensity fluorescent and absorption imaging, turn out to be unreliable when probing a dense atomic packet [7,8]. The former critically depends on the value of the illuminating intensity, the frequency and the repartition of atoms between the different Zeeman sub-levels. The latter poses a problem as soon as the optical depth, proportional to the column density of atoms along the probe direction, is on the order of 3 to 4, because of both (i) the electronic noise of each pixel of the charge-coupled-device (CCD) camera and (ii) the digitalization of the signal of the weak amount of light that remains after the propagation through the cloud.

An optically thick cloud can also be probed with off-resonant light or by implementing the phase contrast imaging technique [7]. The reduction of the scattering cross section that results from the non-resonant probe is favorable. However, the sample becomes dispersive and behaves like a gradient-index lens. Such a technique is fruitful for qualitative or differential measurements, but is difficult to use for quantitative purposes.

To circumvent those drawbacks the group of D. Weiss has successfully implemented a fluorescence imaging technique very far above saturation intensity [3]: the probe intensity was larger by more than three orders of magnitude than the saturation intensity. In this regime,

all atoms, independently of their Zeeman sub-level distribution, spend half of the time in the excited state. This method allows to probe a cloud with a very large optical depth, but requires a dramatically high incident intensity and a subtle alignment of the two counter propagating beam used to drive the fluorescence.

In this article, we report on our realization of a robust, accurate and reliable far above saturation intensity absorption imaging aimed at investigating such dense atomic samples. Its implementation is straightforward and, by contrast with the far above saturation fluorescence imaging technique, the probing does not required the use of a powerful laser.

Indeed, in our experiment, the probe light is provided only by diode lasers. A semiconductor slave laser is injection-locked to a 0.5 MHz linewidth Distributed Bragg Reflector (DBR) master diode laser, and spatially filtered by a pinhole. The purpose of this arrangement is to benefit from a narrow linewidth probe tuned on the transition $^{87}\text{Rb}, 5^2S_{1/2} \rightarrow 5^2P_{3/2}$ while having a relatively large power (30 mW) available to probe the atoms. An acousto-optic modulator placed before the pinhole is used to produce light pulses as short as 250 ns. The shadow cast by the atoms on the resonant probe beam is imaged on a CCD camera, with an optical resolution of $7 \mu\text{m}$.

The response of the atoms, i.e. the population driven in the excited state by the imaging laser beam, depends on the *effective* saturation intensity $I_{\text{eff}}^{\text{sat}} = \alpha^* I_0^{\text{sat}}$, where I_0^{sat} is the saturation intensity for the corresponding two-level transition ($I_0^{\text{sat}} = 1.67 \text{ mW/cm}^2$ for rubidium 87). The dimensionless parameter α^* accounts for corrections due to the specific conditions in which images are taken: the polarization of the imaging beam, the structure of the excited state and the different Zeeman sub-level populations of the degenerate ground state of the optical transition.

In order to extract the spatial atomic density $n(x, y, z)$

of the cloud, we acquire as usual three images: $I_w(x, y)$ with the atoms and probe beam on, $I_{wo}(x, y)$ without the atoms and probe on, and $I_{\text{dark}}(x, y)$ without atoms and probe off. From those images, we work out for each pixel (x, y) , the light intensity $I_f(x, y) = I_w(x, y) - I_{\text{dark}}(x, y)$ (resp. $I_i(x, y) = I_{wo}(x, y) - I_{\text{dark}}(x, y)$) of the imaging beam in presence (resp. absence) of atoms by removing the contribution of the background light illumination taken in the absence of the detection beam.

The Beer's law in presence of saturation effect and for a resonant incident light can be recast in the form:

$$\frac{dI}{dz} = -n \frac{\sigma_0}{\alpha^*} \frac{1}{1 + I/I_{\text{eff}}^{\text{sat}}} I \equiv -n\sigma(I)I \quad (1)$$

where $\sigma_0 = 3\lambda^2/2\pi$ is the resonant cross-section for a two-level atom, and $\sigma(I)$ the effective cross section including saturation correction. From Eq. (1), one readily obtains the expression for the optical depth:

$$od_0(x, y) \equiv \sigma_0 \int n(x, y, z) dz = f(x, y; \alpha^*). \quad (2)$$

where $f(x, y; \alpha^*)$ is defined by:

$$f(x, y; \alpha^*) = -\alpha^* \ln \left(\frac{I_f(x, y)}{I_i(x, y)} \right) + \frac{I_i(x, y) - I_f(x, y)}{I_0^{\text{sat}}}, \quad (3)$$

The optical density is defined by: $\delta_0(x, y) = -\ln(I_f(x, y)/I_i(x, y))$. We have deliberately chosen a definition of the optical depth $od_0(x, y)$ that does not include the parameter α^* so that it depends only on the characteristics of the atomic cloud. However, to extract this quantity from a set of images, one needs to know the parameter α^* .

For low-intensity absorption imaging ($I_i(x, y) \ll I_0^{\text{sat}}$), the optical depth involves only the ratio of the intensities I_f and I_i : $od_0(x, y) \simeq \alpha^* \delta_0(x, y)$. The unknown parameter α^* still needs to be determined independently. The strong saturation imaging technique takes advantage of the reduction of the effective cross-section $\sigma(I)$ when $I \gg \alpha^* I_0^{\text{sat}}$. In this limit, the optical depth depends both on α^* and on the value of the incident intensity $I_i(x, y)$, because of the non-linear atomic response (see Eq. (3)).

The absolute calibration is a crucial but delicate task for fluorescence or low absorption imaging. In the context of our far above saturation absorption imaging technique, it just consists in determining the parameter α^* . We proceed in the following manner. The sample of cold atoms is generated by a compressed elongated two-dimensional MOT. The cloud is imaged after a not too short time-of-flight so that its maximum optical density is not too high (~ 2), which guarantees also the validity of the low-intensity absorption imaging. As the imaging technique is destructive, we acquire several set of images (typically five) of a cloud always prepared in the same conditions for different incident intensities. In practice, we vary the intensity of the imaging beam by more than two orders of magnitude while keeping the

number of photons per pulse constant: the duration of the pulse was varied from 250 ns ($I_i \simeq 23$ mW/cm²) to 100 μ s ($I_i \simeq 0.06$ mW/cm²). Keeping the number of absorbed photons small (~ 5 photons per atom on average) avoids pushing and heating the cloud, thereby changing its characteristics.

In order to infer the value of the dimensionless parameter α^* , we calculate, for different values of the parameter α ranging from 1 to 4, the function $f(x, y; \alpha)$ for the set of images. We extract the amplitude $od(\alpha)$ of those calculated optical depth using a gaussian fit (see Fig. 1). There is only one value α^* of α for which all the calculated $od(\alpha)$ are equal over the whole range of incident intensities. Indeed, od_0 does not depend on the incident probe intensity (see Eq. 2).

In practice, we infer by a least square method the value α^* for which $od(\alpha)$ has a minimum standard deviation over the whole range (more than two orders of magnitude) of incident intensities used to image the cloud (see Fig. 1 inset). We find $\alpha^* = 2.12 \pm 0.1$ and a maximum optical depth $od_0 = 4.8$ that corresponds to an optical density of $\delta_0 = 2.25$ as deduced from the low intensity absorption imaging. We stress that this calibration allows for an absolute determination of the number of atoms, its accuracy being ultimately determined by the calibration of the incident intensity using the CCD array.

This value for α^* is to be compared with the result of the Bloch equations for the corresponding multiple level system. For our data, the atoms are initially in the $|g\rangle = 5^2S_{1/2}, F = 2$ hyperfine state (5-fold degenerated) and the π -polarized probe is resonant with the $|e\rangle = 5^2P_{3/2}, F' = 3$ hyperfine excited state (7-fold degenerated). The probability to excite the $5^2P_{3/2}, F' = 2$ is negligible (below 1 %). The transition $|g\rangle \rightarrow |e\rangle$ can be considered in this limit as closed. From numerical integration of the Bloch equations, we find out that (i) the steady state solution is approximately valid even for the shortest pulses that we use, and (ii) the correction factor α^* to the two-level saturation intensity lies in between one and two depending on the polarization of the probe. Experimentally, the polarization of the beam cannot be perfectly under control because of the slight birefringence of the viewports. In addition, a residual magnetic field may also influence the effective value of α^* .

After calibration, the high-intensity imaging technique is applied to the same cloud but without time-of-flight. The transparency of the atomic cloud is controlled by the probe intensity because of the non-linear response of the atoms. Our numerical studies based on the Eqs. (2) and (3) show that the true profile of the cloud can be reliably inferred from the strong saturation absorption images as soon as the incident intensity of the probe beam is on the order of $I_i \sim \max(od_0) I_{\text{eff}}^{\text{sat}}$. Note that this intensity is much less than the one needed for a reliable high intensity fluorescence imaging technique [3]. We have checked this prediction by imaging with different incident intensities a compressed two-dimensional MOT prepared in the same conditions. To compress the MOT, we proceed

in the following manner: the repumper intensity is divided by 15 in 1 ms, the detuning is ramped linearly from -3Γ to -9Γ in 15 ms, and the gradient is increased from 5 G/cm to 20 G/cm in 15 ms. From our analysis based on the strong saturation absorption, we systematically find out a double structure (see Fig. 2.c) with a central dense region having an maximum peak atomic density on the order of $2(\pm 1) \times 10^{11}$ atoms/cm³ corresponding to $\max(od_0) \sim 45$. Half of the atoms (1.5×10^8) remains in the wing. The profile of those wings and their number of atoms inferred from the low and high intensity absorption imaging techniques perfectly coincides.

In addition, this technique is particularly well suited for the estimation of the spatial extent of dense atomic packets with one or more sizes very small ($\Delta x_0 \leq 30 \mu\text{m}$). If T is the temperature of the cloud, the size of the packet reflects the velocity distribution after a time-of-flight duration on the order of $\tau = (m\Delta x_0^2/k_B T)^{1/2}$. For a cloud of initial size 10 μm and a temperature of 100 μK , $\tau \sim 100 \mu\text{s}$. By contrast with low-intensity absorption imaging, for which the pulse duration is on the order of the time τ , the very short pulse used for high-intensity absorption imaging prevents heating and permits to extract the correct profile.

We have demonstrated a high-intensity absorption imaging technique well-suited for dense, small-size atomic clouds. This technique is robust against small frequency and intensity variations of the probe, and does not require an extremely large probe intensity. We have shown how it can be reliably calibrated exploiting the non-linear atomic response.

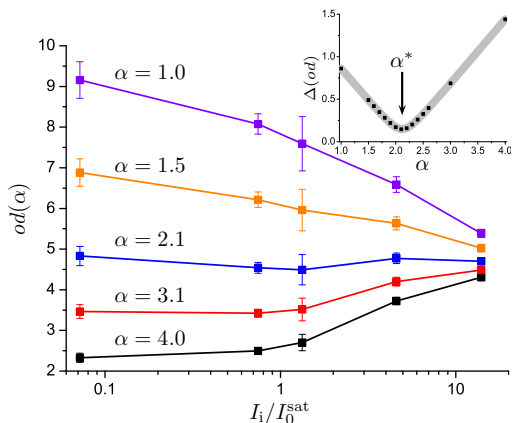


Fig. 1. (color online) A cloud is imaged using different probe intensities (from $I_0^{\text{sat}}/15$ to $15I_0^{\text{sat}}$). For each image, the maximum optical depth of the cloud $od(\alpha)$, deduced from a gaussian fit, is calculated with several values of the unknown parameter α using the function f . The plot represents $od(\alpha)$ as a function of the incoming intensity. The standard deviation $\Delta(od)$ of each set of data points (see inset) exhibits a clear minimum as a function of the parameter α . The minimum of $\Delta(od)$ gives $\alpha^* = 2.12 \pm 0.1$.

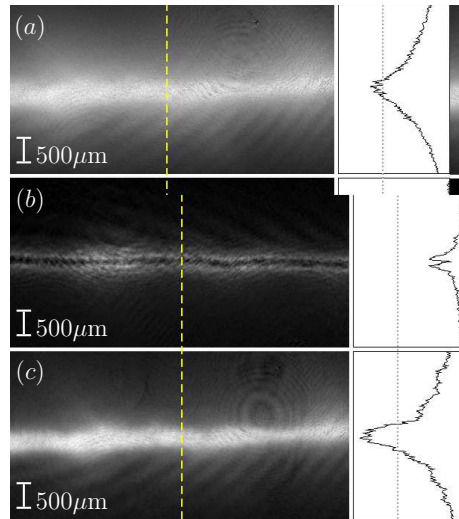


Fig. 2. Three images with a transverse cut of a dense elongated cloud prepared in the same conditions. The transverse profile is given by the dimension less function $f(x, y; \alpha^*)/\alpha^*$ and the dashed line corresponds to the value 3. (a) Low intensity absorption imaging. Almost all the light is absorbed in the center of the cloud. (b) Off-resonance absorption imaging with a probe laser blue-detuned by 1.2Γ where Γ is the natural linewidth of the excited state. One observes a double peak structure resulting from a gradient-index lens effect. (c) High intensity absorption imaging. Only the third method shows that the profile has a double structure, with an r.m.s size for the central peak of 300 μm , corresponding to a peak atomic density $\sim 4(\pm 1) \times 10^{10}$ atoms/cm³ and $\max(od_0) \sim 9$.

We thank J. Dalibard, T. Kawalec and A. Couvert for careful reading of the manuscript. Support for this research came from the Délégation Générale pour l'Armement (DGA) and the Institut Francilien de Recherche sur les Atomes Froids (IFRAF). Z. W. acknowledges support from the European Marie Curie Grant MIF1-CT-2004-509423, and G. R. from the DGA.

References

1. W. Petrich, M. H. Anderson, J. R. Ensher and E. A. Cornell, *J. Opt. Soc. Am. B* **11**, 1332 (1994).
2. C. G. Townsend *et al.*, *Phys. Rev. A*, **52**, 1423 (1995).
3. Marshall T. DePue, S. Luckman Winoto, D. J. Han and David S. Weiss, *Opt. Comm.* **180**, 73 (2000).
4. M. Vengalatorre, R. S. Conroy and M. G. Prentiss, *Phys. Rev. Lett.* **92**, 183001 (2004).
5. T. Kinoshita, T. Wenger, and D. S. Weiss, *Phys. Rev. A* **71**, 011602 (2005).
6. T. Lahaye *et al.*, *Phys. Rev. Lett.* **93**, 093003 (2004).
7. W. Ketterle, D. S. Durfee and D. M. Stamper-Kurn, *Proceedings of the International School of Physics "Enrico Fermi"* (eds M. Inguscio, S. Stringari and C. E. Wieman, IOS Press, 1999) and references therein.

8. S. Kadlecěk, J. Seby, R. Newell, and T. G. Walker, *Opt. Lett.* **26**, 137 (2001).